

Bosonization and functional renormalization group approach in the framework of QED₂

I. Nándori

Institute of Nuclear Research, P.O. Box 51, H-4001 Debrecen, Hungary

(Received 24 August 2010; published 19 September 2011)

Known results on two-dimensional quantum electrodynamics (QED₂) have been used to study the dependence of functional renormalization group equations on renormalization schemes and approximations applied for its bosonized version. It is demonstrated that the singularity of flow equations can be avoided in the optimized and power-law schemes for the bosonized model and the drawback of renormalization on bosonization is shown: it is indicated that renormalization of QED₂ possibly requires interaction terms corresponding to higher frequency modes of its bosonized version.

DOI: [10.1103/PhysRevD.84.065024](https://doi.org/10.1103/PhysRevD.84.065024)

PACS numbers: 11.10.Hi, 11.10.Gh, 11.10.Kk

I. INTRODUCTION

In low dimensions, bosonization rules enable one to reformulate fermionic and gauge models in terms of elementary scalar fields. For example, the bose form of the two-dimensional massive Thirring model [1] is the massless sine-Gordon (SG) scalar theory [2]. Single flavor QED₂ with massive fermions can also be bosonized, and the corresponding scalar theory is the massive sine-Gordon (MSG) model [3–5]. Furthermore, the multiflavor QED₂, and the two-dimensional multicolor quantum chromodynamics (QCD₂) can also be rewritten as multicomponent SG theories [4–6]. Thus, corresponding bose models are usually SG-type theories. The critical behavior of original fermionic and gauge theories and their bosonized versions can be studied by various methods such as renormalization group (RG) approaches. If critical behaviors of fermionic and gauge models are known, then bosonization transformations can be used to consider the dependence of methods suitable for the critical behavior of SG-type models on the approximations used.

The goal of this paper is to study the dependence of functional RG equations obtained for the MSG model on renormalization schemes and applied approximations. The phase structure of the corresponding fermionic theory, the single flavor QED₂ with massive fermions, has already been mapped out by the density matrix RG approach [7], which is used here to optimize the scheme-dependence for the MSG model. The drawback of the RG study of the MSG model on the bosonization transformations is also discussed, namely, it is indicated that renormalization of QED₂ possibly requires interaction terms corresponding to higher frequency modes of the MSG model.

The paper is organized as follows. In Sec. II, some aspects of bosonization are discussed. Functional RG equations are obtained for the MSG model in the second order of the gradient expansion in Sec. III. Results of perturbative RG are summarized briefly in Sec. IV. The nonperturbative RG study is given in Sec. V for the single-frequency, and in Sec. VI for the multifrequency MSG model in local potential approximation (LPA). In Sec. VII, the RG flow is

determined beyond LPA. Section VIII serves as the summary.

II. BOSONIZATION

The mapping of quantum field theories of interacting fermions onto an equivalent theory of interacting bosons called bosonization is well-established in the context of 1 + 1-dimensional theories. The well-known example is the massive Thirring model [1], which is a theory of a single Dirac field ψ determined by the Lagrangian density

$$\mathcal{L}_{\text{Thirring}} = \bar{\psi}(i\gamma^\mu \partial_\mu - m)\psi - \frac{1}{2}g j^\mu j_\mu \quad (1)$$

where $j^\mu = \bar{\psi}\gamma^\mu\psi$, m is the mass, and g is the coupling. This can be mapped onto the SG scalar field theory described by the Lagrangian density [2]

$$\mathcal{L}_{\text{SG}} = \frac{1}{2}(\partial_\mu \varphi)^2 + u \cos(\beta\varphi) \quad (2)$$

where φ is a one-component scalar field and the identifications $4\pi/\beta^2 = 1 + g/\pi$, $-\beta/(2\pi)\epsilon^{\mu\nu}\partial_\nu\varphi = j^\mu$, and $u \cos(\beta\varphi) = -m\bar{\psi}\psi$, are made between the parameters of the two models. (Conventions and the definition for appropriate normal ordering are given in [2].) The Lagrangian of QED₂ with a massive Dirac fermion, which is also called the massive Schwinger model, reads as [3]

$$\mathcal{L}_{\text{QED}_2} = \bar{\psi}(i\gamma^\mu \partial_\mu - m - e\gamma^\mu A_\mu)\psi - \frac{1}{4}F_{\mu\nu}F^{\mu\nu} \quad (3)$$

where $F_{\mu\nu} = \partial_\mu A_\nu - \partial_\nu A_\mu$. Using bosonization technique, the fermionic theory (3) can be mapped onto an equivalent Bose form [3], which is considered as the specific form of the MSG model [4,5,8] whose Lagrangian density is written as

$$\mathcal{L}_{\text{MSG}} = \frac{1}{2}(\partial_\mu \varphi)^2 + \frac{1}{2}M^2\varphi^2 + u \cos(\beta\varphi) \quad (4)$$

with $\beta^2 = 4\pi$, $M^2 = e^2/\pi$, $u = em \exp(\gamma)/(2\pi^{3/2})$ where $\gamma = 0.5774$ is the Euler's constant and the vacuum angle parameter has to be chosen as $\theta = \pm\pi$ for $u > 0$ and

$\theta = 0$ for $u < 0$ [4]. The MSG model has two phases. The Ising-type phase transition [7] is controlled by the dimensionless quantity u/M^2 related to the critical ratio $(m/e)_c$ of QED₂, which separates the confining and the half-asymptotic phases of the fermionic model. The critical ratio $(m/e)_c = 0.31\text{--}0.33$ has been calculated by the density matrix RG method for the fermionic model which implies [7]

$$\left(\frac{u}{M^2}\right)_c = \left(\frac{m}{e}\right)_c \frac{\exp(\gamma)}{2\sqrt{\pi}} = 0.156\text{--}0.168. \quad (5)$$

If one assumes a quartic self-interaction among the massive Dirac fermions of QED₂ by adding a Thirring type term to the Lagrangian (3), then one arrives at the massive Schwinger-Thirring model, which reads as

$$\mathcal{L} = \bar{\psi}(i\gamma^\mu \partial_\mu - m - e\gamma^\mu A_\mu)\psi - \frac{1}{4}F_{\mu\nu}F^{\mu\nu} - \frac{1}{2}g j^\mu j_\mu \quad (6)$$

where $F_{\mu\nu} = \partial_\mu A_\nu - \partial_\nu A_\mu$ and $j^\mu = \bar{\psi}\gamma^\mu\psi$. It has been argued that by using bosonization technique the fermionic theory (6) can be mapped onto the MSG model if $4\pi/\beta^2 = 1 + g/(2\pi)$ and the Fourier amplitude is related to the fermion mass ($u \sim m$) and $M^2 = e^2/(\pi + g/2)$. Let us note that the bosonization of two-dimensional gauge and fermionic models (special attention on the Schwinger-Thirring model) has been the subject of intense study [9].

III. FUNCTIONAL RG METHOD FOR THE MSG MODEL

In this section, we derive functional RG equations for the MSG model. Recently, the complete phase structure of the SG model (2) has been mapped out by extending the functional RG analysis [10] beyond LPA [11]. Here we use the same RG approach for the MSG model (4). Namely, the effective average action functional RG method [12–14] where the evolution equation reads as

$$k\partial_k\Gamma_k = \frac{1}{2}\text{Tr}[(R_k + \Gamma_k'')^{-1}k\partial_k R_k] \quad (7)$$

with the notation $' = \partial/\partial\varphi$, and the trace Tr stands for the integration over all momenta. As exact RG Eqs. (7) are functional equations they are handled by truncations. Truncated RG flows depend on the choice of the regulator function R_k , i.e., on the renormalization scheme. In order to optimize the scheme-dependence, various strategies have been worked out. For example, a general optimization procedure was proposed to increase the convergence of the truncated flow [15], and successfully applied in many cases, e.g., in quantum gravity [16] or in low-energy QCD [17]. Although, the optimized regulator R_k^{opt} [15] does not support the gradient expansion beyond second order, but an optimization criterion based on functional variation is proposed to handle this problem [20] and has been used for

the study of low-energy behavior of the Yang-Mills theory. Since the RG study of the SG model was done by using the power-law type regulator R_k^{pow} [13], it is a natural choice that for the RG analysis of the MSG model we use also the power-law regulator and the previously mentioned optimized one

$$R_k^{\text{pow}} = p^2\left(\frac{k^2}{p^2}\right)^b, \quad R_k^{\text{opt}} = a(k^2 - p^2)\Theta(k^2 - p^2) \quad (8)$$

where $b \geq 1$, usually $a = 1$ and $\Theta(x)$ is the Heaviside step-function. Let us note that various types of regulator functions can be used (e.g., the exponential one [12]), but here we focus on those (8) which provide us the possibility to perform momentum integrals of RG equations analytically.

Another problem related to truncations is the singularity of RG flows. The appearance of spinodal instability (SI), i.e., singularity in the RG flow could be the consequence of a too drastic truncation. In this work, we show that the singularity of the RG flow obtained for the MSG model can be avoided for the optimized and power-law regulators (8), if the RG equation obtained in LPA is integrated out directly, i.e., using appropriate approximations, the effective potential remains convex [21]. Let us note that the MSG model has already been investigated by using the truncated Fourier expansion of the potential which was found to be a too drastic simplifications of the functional subspace since SI appeared in the RG flow and the Maxwell construction resulted in a degenerate effective potential scheme independently [8].

Equation (7) has been solved over the functional subspace spanned by the ansatz for the MSG model (4)

$$\Gamma_k = \int_x \left[\frac{1}{2}z(\partial_\mu \varphi_x)^2 + V_k(\varphi_x) \right], \quad (9)$$

where the local potential contains a single Fourier mode

$$V_k(\varphi) = \frac{1}{2}\mathbf{M}^2(k)\varphi^2 + u(k)\cos(\varphi), \quad (10)$$

and the following notations are introduced

$$\mathbf{M}^2 \equiv zM^2, \quad z \equiv 1/\beta^2 \quad (11)$$

via the rescaling of the field $\varphi \rightarrow \varphi/\beta$ in (4) and $z(k)$ stands for the field-independent wave-function renormalization. Although RG transformations generate higher harmonics, we use the simple ansatz (10) first since in the case of the SG model it was found to be an appropriate approximation [11]. Then Eq. (7) leads to the evolution equations [11]

$$\partial_k V_k = \frac{1}{2} \int_p \mathcal{D}_k k \partial_k R_k, \quad (12)$$

$$k\partial_k z = \mathcal{P}_0 V_k''' \int_p \mathcal{D}_k^2 k \partial_k R_k \left(\frac{\partial^2 \mathcal{D}_k}{\partial p^2 \partial p^2} p^2 + \frac{\partial \mathcal{D}_k}{\partial p^2} \right) \quad (13)$$

with $\mathcal{D}_k = 1/(z p^2 + R_k + V_k'')$ and $\mathcal{P}_0 = (2\pi)^{-1} \int_0^{2\pi} d\varphi$ as the projection onto the field-independent subspace. The scale k covers the momentum interval from the UV cutoff Λ to zero. Inserting the ansatz (10) into Eqs. (12) and (13), the flow equations for the coupling constants are (similar RG equations obtained for the SG model in [10])

$$k\partial_k u = \frac{1}{2\pi} \int_p \frac{p(k\partial_k R_k)}{u} \left(\frac{P}{\sqrt{P^2 - u^2}} - 1 \right), \quad (14)$$

$$k\partial_k z = \frac{1}{2\pi} \int_p p(k\partial_k R_k) \left(\frac{u^2 p^2 (\partial_{p^2} P)^2 (4P^2 + u^2)}{4(P^2 - u^2)^{7/2}} - \frac{u^2 P (\partial_{p^2} P + p^2 \partial_{p^2}^2 P)}{2(P^2 - u^2)^{5/2}} \right) \quad (15)$$

with $P = z p^2 + \mathbf{M}^2 + R_k$ where $\partial_k \mathbf{M} = 0$. In general, the momentum integrals have to be performed numerically, however, in some cases analytical results are available. Indeed, by using the power-law type regulator function with $b = 1$ (i.e., the Callan-Symanzik scheme), the momentum integrals can be performed and the RG equations reads as,

$$(2 + k\partial_k)\tilde{u} = \frac{1}{2\pi z \tilde{u}} \left[1 + \tilde{\mathbf{M}}^2 - \sqrt{(1 + \tilde{\mathbf{M}}^2)^2 - \tilde{u}^2} \right]$$

$$k\partial_k z = -\frac{1}{24\pi} \frac{\tilde{u}^2}{[(1 + \tilde{\mathbf{M}}^2)^2 - \tilde{u}^2]^{(3/2)}}$$

$$(2 + k\partial_k)\tilde{\mathbf{M}}^2 = 0, \quad (16)$$

with dimensionless couplings $\tilde{u} = k^{-2}u$, $\tilde{\mathbf{M}}^2 = k^{-2}\mathbf{M}^2$.

IV. PERTURBATIVE RG

Let us first consider the massless limit ($\tilde{\mathbf{M}} \rightarrow 0$) when the RG Eqs. (16) reduce to those derived for the SG model [11]. The spontaneously broken phase of the SG model is known to be equivalent to the neutral sector of the massive Thirring model (1). Indeed, the renormalization of the massive Thirring model has already been discussed, and it was demonstrated that the scaling of the fermion mass (see, e.g., [22]), $m = m_0(\mu/\Lambda)^{-(g/(g+\pi))}$ is identical to the solution of the linearized form of the RG Eqs. (16) if $k\partial_k z = 0$ and $\tilde{\mathbf{M}} = 0$ are assumed and the equivalences $g/(g + \pi) = 1 - 1/(z4\pi)$, $k = \mu$, $u = m\mu/\pi$, and $u_\Lambda = m_0\Lambda/\pi$ are used.

For nonvanishing mass ($\tilde{\mathbf{M}} \neq 0$), it is illustrative to compare the perturbative RG equations given in [23,24] to that obtained by the linearization of Eq. (16), which reads as

$$(2 + k\partial_k)\tilde{u} = \frac{1}{4\pi} \frac{\tilde{u}}{z} \frac{1}{1 + \tilde{\mathbf{M}}^2} + \mathcal{O}(\tilde{u}^2)$$

$$k\partial_k z = -\frac{1}{24\pi} \tilde{u}^2 \frac{1}{(1 + \tilde{\mathbf{M}}^2)^3} + \mathcal{O}(\tilde{u}^3)$$

$$(2 + k\partial_k)\tilde{\mathbf{M}}^2 = 0. \quad (17)$$

Let us relate the parameters of [23] μ , κ , and m^2 to that of defined in Eqs. (9) and (10), namely $u = \mu$, $z = 1/(4\pi^2\kappa)$, $\mathbf{M}^2 = m^2/(4\pi\kappa)$, and $k = \Lambda$. By using these equivalences, the approximated RG equations (3.17) of [23] can be written as

$$(2 + k\partial_k)\tilde{u} = \frac{1}{4\pi} \frac{\tilde{u}}{z} \frac{z}{z + \tilde{\mathbf{M}}^2} + \frac{1}{16\pi} \frac{\tilde{u}^3}{z^3} \left(\frac{z}{z + \tilde{\mathbf{M}}^2} \right)^3$$

$$k\partial_k z = -\frac{\alpha_2}{8} \frac{\tilde{u}^2}{z} \frac{z}{z + \tilde{\mathbf{M}}^2} \quad (2 + k\partial_k)\tilde{\mathbf{M}}^2 = 0, \quad (18)$$

with α_2 constant. Perturbative results (Eqs. (17) and (18)) demonstrate that the Kosterlitz-Thouless-Berezinski (KTB)-[25] type phase transition known to take place for the SG theory [10], disappears in case of the MSG model. Indeed, one expects an Ising-type second order phase transition for the MSG scalar model, which is controlled by the dimensionless ratio $u/M^2 = \tilde{u}/\tilde{\mathbf{M}}^2$. For example, according to Eq. (17), in the infrared (IR) limit ($k \rightarrow 0$) the mass term becomes large $\tilde{\mathbf{M}}^2 \sim k^{-2}$, which freezes out the evolution of z and the Fourier amplitude has a trivial tree-level scaling $\tilde{u} \sim k^{-2}$; consequently, the ratio $\tilde{u}/\tilde{\mathbf{M}}^2$ tends to a constant value.

However, the perturbative RG flow produces arbitrary large ratio depending on the initial conditions (there is no upper bound), hence no critical value can be determined. Consequently, the perturbative RG flow is not suitable for the prediction of the Ising-type phase transition of the MSG model.

V. FUNCTIONAL RG STUDY OF THE SINGLE-FREQUENCY MSG MODEL

Exact RG equations (with a single Fourier mode) show a different picture since one cannot obtain arbitrary large IR value for the ratio $\tilde{u}/\tilde{\mathbf{M}}^2$. Let us first consider the RG flow obtained by the optimized regulator function (8) with $a = 1$ in the LPA (i.e., $z = 1/\beta^2 = \text{constant}$), which reads as

$$(2 + k\partial_k)\tilde{u} = -\frac{1}{2\pi\beta^2\tilde{u}} \left[1 - \sqrt{\frac{(1 + \tilde{\mathbf{M}}^2)^2}{(1 + \tilde{\mathbf{M}}^2)^2 + \beta^4\tilde{u}^2}} \right],$$

$$(2 + k\partial_k)\tilde{\mathbf{M}}^2 = 0. \quad (19)$$

In the broken symmetric phase, the RG trajectories merge into a single trajectory in the deep IR region, which is characterized by the critical ratio $[\tilde{u}/\tilde{\mathbf{M}}^2]_c = 0.0625$ (for $\beta^2 = 4\pi$) and serves as an upper bound (see Fig. 1). The

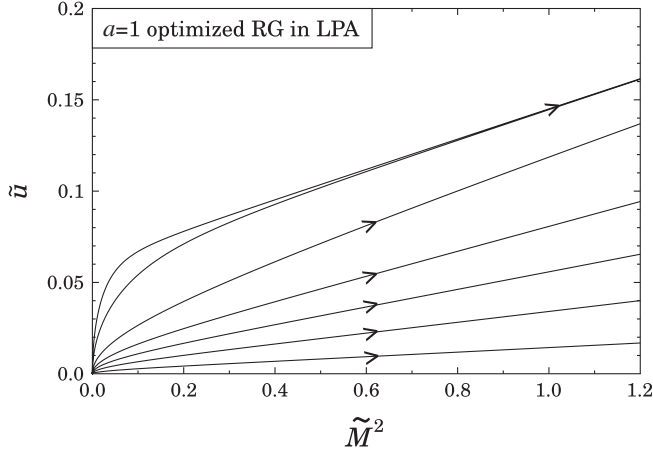


FIG. 1. Phase diagram of the MSG model for $\beta^2 = 4\pi$. RG trajectories are obtained by the integration of Eq. (19). Since SI does not occur in the RG flow, the critical ratio of the MSG model can be determined, $[\tilde{u}/\tilde{M}^2]_c = 0.0625$. The arrows indicate the direction of the flow.

critical value obtained by Eq. (19) is less than the exact result (5), therefore it requires further improvement. Let us try to improve it by the optimized regulator (8) with $a \neq 1$, which has the following form in LPA

$$(2 + k\partial_k)\tilde{u} = \frac{a}{(a-1)2\pi\tilde{u}\beta^2} \left[(1 + \tilde{M}^2) - (a + \tilde{M}^2) + \sqrt{(a + \tilde{M}^2)^2 - \tilde{u}^2\beta^4} - \sqrt{(1 + \tilde{M}^2)^2 - \tilde{u}^2\beta^4} \right],$$

$$(2 + k\partial_k)\tilde{M}^2 = 0. \quad (20)$$

However, for $a \neq 1$, spinodal instability (SI) appears in the RG flow in the broken symmetric phase, i.e., RG equations become singular in the IR limit and the RG flow stops at some finite scale (see the dashed lines in Fig. 2.) Although RG trajectories start to converge into a single one in the broken phase the critical value of the single-frequency MSG model cannot be determined unambiguously. In other words, the convergence properties of the optimized RG is weakened for $a \neq 1$. Let us try to use other types of RG equations, for example, the power-law type RG with $b = 1$ in LPA which reads as

$$(2 + k\partial_k)\tilde{u} = \frac{(1 + \tilde{M}^2) - \sqrt{(1 + \tilde{M}^2)^2 - \tilde{u}^2\beta^4}}{2\pi\tilde{u}\beta^2},$$

$$(2 + k\partial_k)\tilde{M}^2 = 0. \quad (21)$$

The RG Eq. (21) can be obtained by rescaling $\tilde{u} \rightarrow \tilde{u}/z$ and $\tilde{M}^2 \rightarrow \tilde{M}^2/z$ in (16) and using the identifications (11) with the assumption $\partial_k z = 0$. It is known that in the sharp

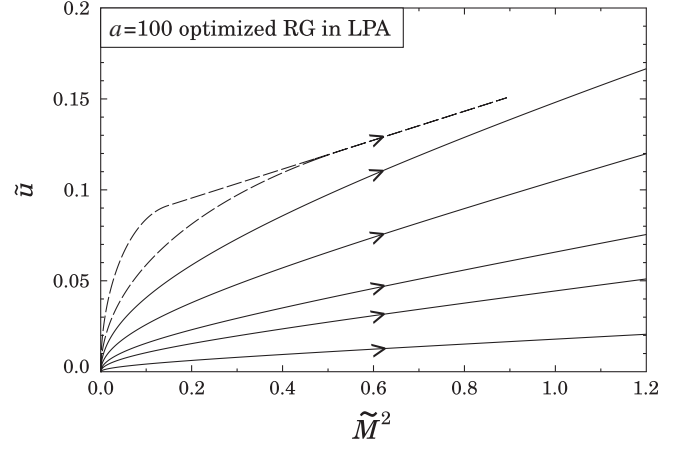


FIG. 2. Phase diagram of the MSG model for $\beta^2 = 4\pi$. RG trajectories are obtained by the integration of Eq. (20) with $a = 100$. The dashed lines correspond to RG trajectories where SI occurs in the RG flow, thus the critical ratio of the MSG model cannot be obtained.

limit, the optimized RG becomes identical to the power-law type RG with $b = 1$, i.e., Eq. (20) reduces to Eq. (21) for $a \rightarrow \infty$. Thus, SI is expected in case of Eq. (21). Indeed, the numerical solution of (21) indicates the appearance of SI in the broken symmetric phase (see the dashed lines in Fig. 3.)

It is also illustrative to compare the IR values of the ratio \tilde{u}/\tilde{M}^2 at the scale of SI given by the integration of optimized RG with various values for the parameter a using the same UV initial condition (see Fig. 4.) This demonstrates that the best estimate for the critical ratio of the single-frequency MSG model, in the framework of the optimized RG, can be achieved for $a = 1$. Our findings are consistent to the feature of the optimized RG, namely, that it increases

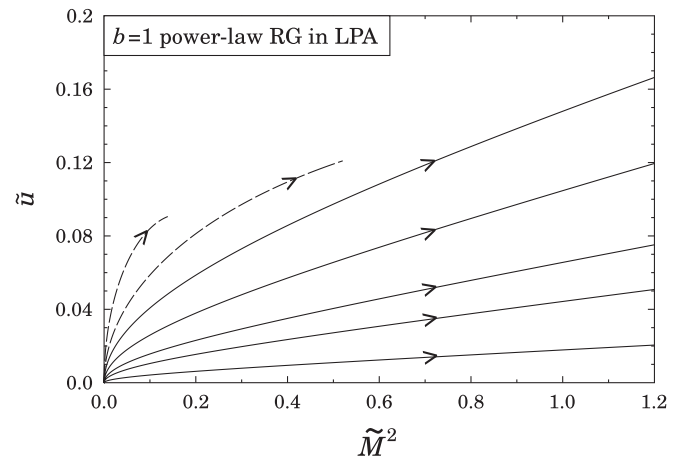


FIG. 3. Phase diagram of the MSG model for $\beta^2 = 4\pi$. RG trajectories are obtained by the integration of Eq. (21). The dashed lines correspond to RG trajectories where SI occurs in the RG flow, thus the critical ratio of the single-frequency MSG model cannot be obtained.

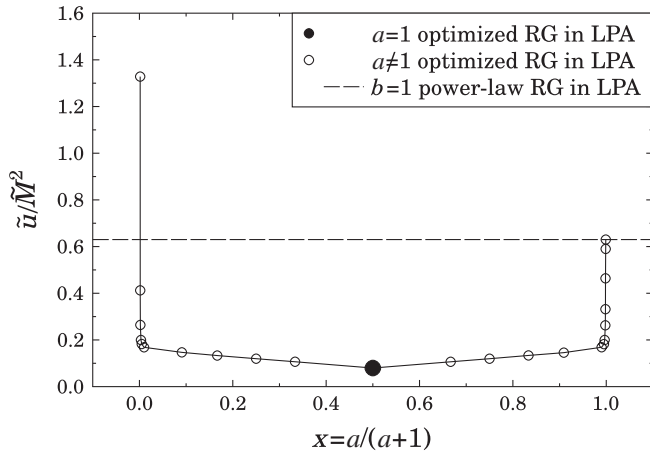


FIG. 4. This figure shows how the IR value of the ratio \tilde{u}/\tilde{M}^2 obtained by the integration of RG Eqs. (19) and (20) depends on the parameter a of the regulator function. The same initial condition has been used for the numerical integration, ($\tilde{u}(\Lambda) = 10^{-5}$, $\tilde{M}^2(\Lambda) = 10^{-9}$). SI has occurred for $a \neq 1$, thus the RG flow stops at some finite scale where the ratio has been read off and plotted. It is possible to avoid SI but only for $a = 1$. For $a \rightarrow \infty$ (i.e., $x \rightarrow 1$) the RG Eq. (20) becomes identical to that that was obtained by the power-law type regulator with $b = 1$ (21); consequently in this case the IR values of the ratio coincide.

the convergence properties of the truncated flow. For example, a similar result is shown in Fig. 12 of [26] in the framework of the $O(N)$ symmetric scalar theory in $d = 3$ dimensions, which has been the subject of intense study on scheme-dependence (see, e.g., [27]). Let us note that the optimized RG with $a = 1$ produces reliable results for the single-frequency MSG model in LPA as opposed to the Wilson-Polchinski RG [28], which was found to be inappropriate [8] for the determination of the phase structure of the MSG model. This is a counterexample for the statement, namely, that the Wilson-Polchinski RG and the optimized one always provide us with the same critical behavior in LPA [18]. The mapping between the two latter RG methods works only if the potential is nondegenerate, but this is not true for the broken symmetric phase of the MSG model.

Since Eq. (19) has no singular behavior, the appearance of SI is expected to be the consequence of an inappropriate approximation, e.g., too drastic simplification of the functional subspace. Let us also note that SG-type models undergo an infinite order (or topological) phase transition, and it was shown [11] that the study of a single-frequency model is sufficient to recover the KTB-type critical properties (higher harmonics were found to be irrelevant). However, the MSG model has an Ising-type second order phase transition, hence there is no reason to focus on the study of a single-frequency model. Consequently, in order to obtain reliable results and to avoid SI in case of the MSG model, one has to incorporate higher harmonics generated by RG Eqs. (12) and (13), which is discussed in the next section.

VI. FUNCTIONAL RG STUDY OF THE MULTI-FREQUENCY MSG MODEL

We now turn to the discussion of the MSG model including higher harmonics. Let us consider the RG Eq. (12) in LPA (i.e., $\partial_k z = 0$) using the ansatz

$$V_k(\varphi) = \frac{1}{2} M^2 \varphi^2 + \sum_{n=1}^{\infty} u_n(k) \cos(n\beta\varphi). \quad (22)$$

There are two ways to determine the IR scaling of the MSG model: (i) either the partial differential Eq. (12) has to be solved directly by, e.g., a computer algebraic program using the initial condition (4) (higher harmonics are generated by RG equations), (ii) or one can find the solution of ordinary differential equations given for the coupling constants which are obtained by inserting the ansatz (22) into Eq. (12). Let us first discuss the latter case when it is unavoidable to implement a further approximation besides the LPA, namely, the truncation of the Fourier expansion of the potential. In this case, the RG flow on the trajectories started at $\beta^2 = 4\pi$ in the broken symmetric phase develops SI at some finite scale $k_{\text{SI}} > M$ [8]. The way to go beyond k_{SI} is the Maxwell construction (i.e., the tree-level blocking relation [29]), which represents too strong constraint on the RG flow and results in a scheme-independent infrared value for the critical ratio $[\tilde{u}/\tilde{M}^2]_c = 0.159$ [8]. However, SI occurs in the RG flow as an artifact [8,30] due to the truncated Fourier-expansion applied to the almost degenerate blocked action of the MSG model, thus, one has to solve directly the RG Eq. (12) in order to obtain reliable results.

Indeed, the truncation of the expansion of the blocked potential in a series of base functions may become unreliable when the blocked action becomes almost degenerate, i.e., when $k^2 + V_k''$ approaches zero [30]. This motivates a direct numerical solution of the RG Eq. (12) for the

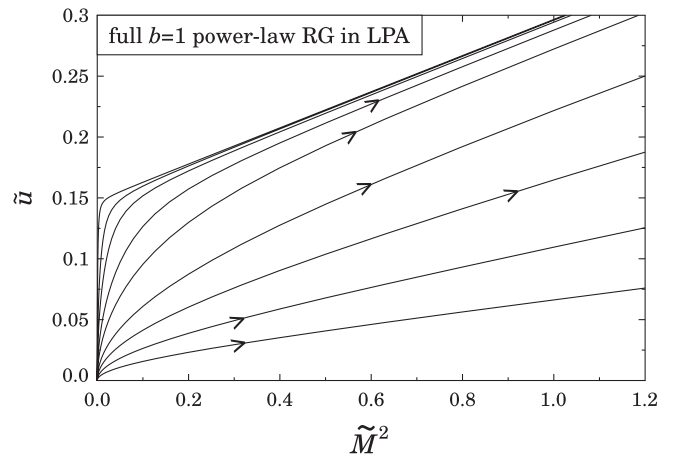


FIG. 5. Phase diagram of the MSG model for $\beta^2 = 4\pi$. RG trajectories are obtained by the direct numerical solution of Eq. (23) (solid lines) incorporating the effect of higher harmonics.

TABLE I. Critical ratio obtained by various RG methods.

opt. single-fr.	opt. multi-fr.	$b = 1$ multi-fr.	$b = 2$ multi-fr.
0.062	0.159	0.148	0.159

blocked potential, which avoids any assumption on the functional subspace where the solution is sought for and any truncated series expansion in some base functions. In this case, the appearance of SI is avoided and the critical ratio can be determined scheme-dependently. For example, Eq. (12) for the power-law type regulator with $b = 1$ reads as

$$(2 + k\partial_k)\tilde{V}_k(\varphi) = -\frac{1}{4\pi} \ln(1 + \tilde{V}_k''(\varphi)) \quad (23)$$

of which direct integration results in $[\tilde{u}/\tilde{M}^2]_c = 0.148$ (see the solid lines in Fig. 5). Moreover, one obtains a better result $[\tilde{u}/\tilde{M}^2]_c = 0.159$ for the optimized regulator and also for the power-law type one with $b = 2$. Consequently, in case of the direct integration of RG equations (when the effect of higher harmonics are incorporated), (i) SI can be avoided in the RG flow, (ii) the critical ratio is found to be scheme-dependent, (iii) the RG schemes can be optimized using the known result (5) obtained for QED₂. Let us note that the best result for the critical ratio (the maximum which can be achieved by any RG scheme in LPA) is obtained by regulators which have good convergence properties, e.g., in case of the optimized RG one has to choose $a = 1$ and for the power-law RG the good choice is $b > 1$. Those regulators which provide for RG equations poor convergence properties like the optimized regulator with $a \neq 1$ and the power-law type regulator with $b = 1$ are not suitable to recover the best result for the critical ratio. For comparison, see Table I.

VII. FUNCTIONAL RG BEYOND THE LPA

Can the appearance of SI be avoided by the inclusion of the wave-function renormalization? What is the IR value for the frequency (i.e., $\beta^2 = 1/z$) in the broken symmetric phase of the MSG model if the wave-function renormalization is included? How does the wave-function renormalization affect bosonization? In order to clarify these issues, let us go beyond the LPA and solve the flow Eqs. (14) and (15) obtained for the single-frequency MSG model where the wave-function renormalization z is kept scale-dependent. Since the optimized regulator does not support the derivative expansion beyond second order in this section, we focus on the power-law RG.

Let us first consider the Callan-Symanzik scheme (i.e., the power-law RG with $b = 1$) where the flow Eqs. (14) and (15) reduce to Eq. (16). As is seen in the inset of Fig. 6, SI appears in the RG flow in the broken symmetric phase, i.e., the RG equation becomes singular in the IR limit and

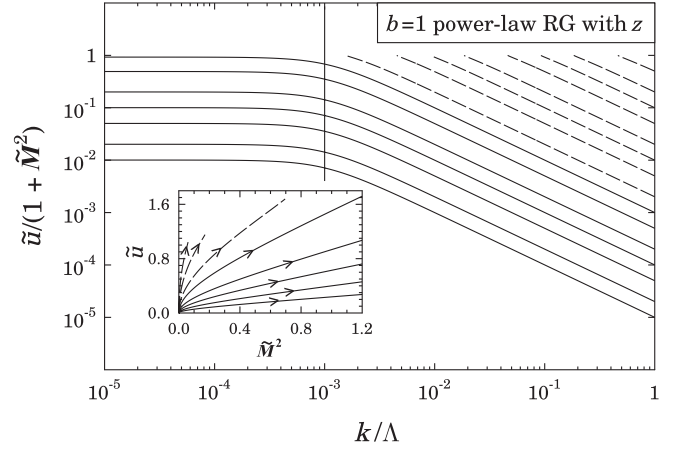


FIG. 6. RG trajectories are obtained by the integration of Eq. (16). Dashed lines correspond to RG trajectories where SI occurs, thus the critical ratio $r_{b=1}^c$ cannot be determined unambiguously. Vertical line shows the dimensionful mass scale, which remains unchanged under RG transformations.

the flow stops at some finite momentum scale (see the dashed lines in the inset of Fig. 6.)

Since the convergence properties of the power-law RG are increased for $b > 1$, Eqs. (14) and (15) are solved numerically for $b = 2$ (see Fig. 7.) Independently of the actual value of b , the potential was found to become degenerate in the broken symmetric phase and the RG flow is determined by the degeneracy condition (similar results were obtained for the SG model in [11])

$$c(b)z^{1-1/b} - \tilde{u} + \tilde{M}^2 = 0 \quad (24)$$

where $c(b) = b/(b-1)^{1-1/b}$. Therefore, in the IR limit the ratio

$$r_b(k) = \frac{\tilde{u}}{c(b)z^{1-1/b} + \tilde{M}^2} \quad (25)$$

tends to one (i.e., $r_b(k \rightarrow 0) = 1$) in the broken phase (see the dashed lines in Fig. 7 for $b = 2$). Therefore, the ratio becomes universal in the broken phase. In the symmetric phase, it tends to a constant IR value depending on the initial conditions. The critical ratio $r_b^c(k)$, which separates the phases of the single-frequency MSG model, is represented by the thick solid line in Fig. 7. Similar results can be obtained for $b = 1$ (see the dashed lines in Fig. 6), but due to the poor convergence properties of the Callan-Symanzik scheme, SI appears in the RG flow in the broken symmetric phase, and the ratio cannot reach its universal value. Let us note that the RG flow always stops at a finite momentum scale in the broken phase independently of b , but a better convergence is obtained for $b > 1$. This indicates that a more accurate calculation requires the inclusion of higher harmonics as it was demonstrated in LPA.

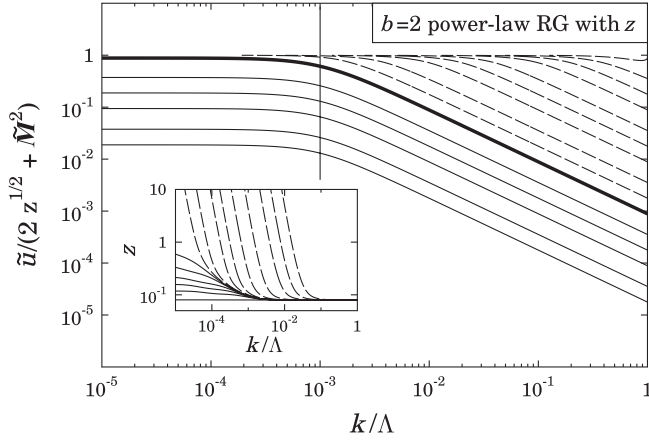


FIG. 7. RG trajectories are obtained by the numerical integration of Eqs. (14) and (15) for the power-law regulator with $b = 2$. Dashed lines correspond to RG trajectories in the broken symmetric phase of the single-frequency MSG model. Vertical line shows the dimensionful mass scale, which remains unchanged under RG transformations. The inset shows the scaling of the wave-function renormalization in the two phases.

In general, the single-frequency approximation is “improved” by the inclusion of the wave-function renormalization. For example, the critical exponent ν of the MSG model can be obtained in the framework of the power-law RG with $b > 1$ if $z(k)$ is kept scale-dependent. It is known [7] that the MSG model belongs to the two-dimensional Ising universality class, thus the correlation length is a power-law function of the reduced temperature $\xi \sim t^{-\nu}$ with $\nu = 1$. Indeed, if one defines the correlation length in the symmetric (disordered) phase by the constant IR values of the ratio, $\xi \sim [1 - r_b(k \rightarrow 0)]^{-1}$ and the reduced temperature is given by the initial UV ($k = \Lambda$) values, $t = [r_b(\Lambda)^{-1} - r_b^c(\Lambda)^{-1}]/r_b^c(\Lambda)^{-1}$ then $\nu = 1$ is obtained (see solid lines in Fig. 7 for $b = 2$). Let us note that in following Ref. [11] the correlation length can be defined as $\xi \sim (\mathbf{M} - k_c)^{-1}$ in the broken phase where k_c represents the momentum scale at which the ratio (25) becomes constant during the RG flow. If the reduced temperature is $t = [r_b(\Lambda) - r_b^c(\Lambda)]/r_b^c(\Lambda)$ then one obtains again the power-law behavior with $\nu = 1$. Consequently, the RG equations derived for the single-frequency MSG model beyond LPA are sufficient to indicate that the model undergoes a second order Ising-type phase transition (while it is known that the SG model has an infinite order, KTB-type phase transition [11]).

Let us consider the RG evolution of the wave-function renormalization, which is equivalent to the inverse frequency, i.e., $z(k) \equiv 1/\beta^2(k)$. In the symmetric phase, $z(k)$ becomes a constant in the IR limit depending on the initial conditions (see the solid lines in the inset of Fig. 7.) In the broken symmetric phase, however, $z(k)$ runs into infinity for $k \rightarrow 0$ (see dashed lines in the inset of Fig. 7), i.e., it has a universal behavior in the broken phase thus

$\beta(k)$ tends to zero. Therefore, if one assumes that bosonization identifications between the parameters of the fermionic and the corresponding bosonic theory hold also for the blocked action, then our result has a drawback on bosonization, namely, it indicates the necessity to construct the fermionic counterpart of the MSG model for $\beta^2 \neq 4\pi$.

Finally, let us mention an open question related to the renormalization of the MSG model. By the inclusion of the wave-function renormalization, it was possible to determine the critical exponent of the correlation function, which demonstrates that the MSG model belongs to the universality class of the two-dimensional Ising model, i.e., the $O(N)$ symmetric scalar theory for $N = 1$ and $d = 2$. It is known that higher order polynomial terms are needed in case of the $O(1)$ model in order to obtain the critical behavior of the MSG model found at the IR limit is the consequence of a Wilson-Fisher type fixed point, which could possibly appear in the MSG model if higher polynomials of the field are incorporated in the RG flow. Therefore, it is an interesting open question to consider the phase structure of the MSG model with the inclusion of higher order monomials of the field, although these terms are not generated by RG equations using the ansatz (4).

VIII. CONCLUSIONS

Known results on QED₂ have been used to optimize RG schemes for its bosonized version, the MSG model, and to consider how the results obtained by RG equations depend on various approximations used. By the inclusion of the wave-function renormalization and the direct integration of RG equations derived for the MSG model, we went beyond the previously used approximations.

It was shown that the inclusion of higher harmonics and the direct integration of RG equations are both needed to avoid the appearance of singularity in the RG flow of the MSG model (for the optimized and power-law regulators) and to recover the critical ratio of QED₂. It is also demonstrated that the optimized RG predicts a reliable result for the single-frequency MSG model in LPA and it is known that the Wilson-Polchinski flow is not suitable to map out its phase structure [8]. Thus, it shows that the two latter RG methods do not produce the same critical behavior in LPA if the blocked potential becomes degenerate, which is the case for the MSG model in its broken phase.

Moreover, as a result of optimization, the best result for the critical ratio of QED₂ (the maximum which can be reached in LPA) is obtained by those regulators which have good convergence properties, such as the optimized RG with $a = 1$ and the power-law RG with $b > 1$. Regulators with poor convergence properties (e.g., optimized RG with $a > 1$ and power-law RG with $b = 1$) are found to be unable to recover the best result.

If one assumes that the identifications between the parameters of the fermionic and the corresponding bosonic theory holds also for the blocked action, then results on the MSG model indicate that the renormalization of QED_2 possibly require interaction terms which correspond to higher frequency modes of its bosonized version. The renormalization of the wave function in the RG flow of the MSG model has also a drawback on bosonization. Since in this case $z = 1/\beta^2$ is scale-dependent, it is a necessity to construct the fermionic counterpart of the MSG model for $\beta^2 \neq 4\pi$. Indeed, if one assumes a quartic self-interaction among the massive Dirac fermions of QED_2 by adding a Thirring-type term to the Lagrangian (3), then one arrives at the massive Schwinger-Thirring model (6), which was proposed as the corresponding fermionic theory of the MSG model for $\beta^2 \neq 4\pi$.

Finally, let us note that the scenario discussed in this work can possibly be extended for many-body condensed

matter systems [31]. Another open question related to the present work is the direct comparison between flows of fermionic and bosonic models. For example, one can try to compare the functional RG study of the SG scalar theory and the fermionic Thirring model, which can possibly be achieved by the extension of the RG analysis of the three-dimensional Thirring model [32] to the two-dimensional one. Furthermore, bosonized versions of multiflavor QED_2 and multicolor QCD_2 are also SG-type models, hence they represent further examples where the drawback of RG results can be studied on bosonization (including wavefunction renormalization as the frequency becomes scale-dependent).

ACKNOWLEDGMENTS

This research was supported by the TÁMOP 4.2.1./B-09/1/KONV-2010-0007 project.

-
- [1] W. Thirring, *Ann. Phys. (N.Y.)* **3**, 91 (1958).
 [2] S. R. Coleman, *Phys. Rev. D* **11**, 2088 (1975).
 [3] S. R. Coleman, R. Jackiw, and L. Susskind, *Ann. Phys. (N.Y.)* **93**, 267 (1975).
 [4] I. Nándori, *Phys. Lett. B* **662**, 302 (2008).
 [5] S. Nagy, J. Polonyi, and K. Sailer, *Phys. Rev. D* **70**, 105023 (2004); I. Nándori, S. Nagy, K. Sailer, and U. D. Jentschura, *Nucl. Phys. B* **725**, 467 (2005); I. Nándori, *J. Phys. A* **39**, 8119 (2006); S. Nagy, I. Nándori, J. Polonyi, and K. Sailer, *Phys. Rev. D* **77**, 025026 (2008); S. Nagy, *Phys. Rev. D* **79**, 045004 (2009).
 [6] J. Kovács, S. Nagy, I. Nándori, and K. Sailer, *J. High Energy Phys.* **01** (2011) 126.
 [7] T. M. Byrnes, P. Sriganesh, R. J. Bursill, and C. J. Hamer, *Phys. Rev. D* **66**, 013002 (2002).
 [8] I. Nándori, S. Nagy, K. Sailer, and A. Trombettoni, *Phys. Rev. D* **80**, 025008 (2009).
 [9] J. Föhlich and E. Seiler, *Helv. Phys. Acta* **49**, 889 (1976); L. V. Belvedere, A. de Souza Dutra, C. P. Natividade, and A. F. de Queiroz, *Ann. Phys. (N.Y.)* **296**, 98 (2002); E. M. C. Abreu, D. Dalmazi, A. de Souza Dutra, and Marcelo Hott, *Phys. Rev. D* **65**, 125030 (2002); D. Dalmazi and A. de Souza Dutra, *J. Phys. A* **40**, 13479 (2007); G. Benfatto, P. Falco, and V. Mastropietro, *Commun. Math. Phys.* **285**, 713 (2008);
 [10] I. Nándori, J. Polonyi, and K. Sailer, *Phys. Rev. D* **63**, 045022 (2001); I. Nándori, K. Sailer, U. D. Jentschura, and G. Soff, *Phys. Rev. D* **69**, 025004 (2004); S. Nagy, K. Sailer, and J. Polonyi, *J. Phys. A* **39**, 8105 (2006); S. Nagy, I. Nándori, J. Polonyi, and K. Sailer, *Phys. Lett. B* **647**, 152 (2007).
 [11] S. Nagy, I. Nándori, K. Sailer, and J. Polonyi, *Phys. Rev. Lett.* **102**, 241603 (2009); S. Nagy and K. Sailer, arXiv:1012.3007.
 [12] C. Wetterich, *Nucl. Phys. B* **352**, 529 (1991); *Phys. Lett. B* **301**, 90 (1993).
 [13] T. R. Morris, *Int. J. Mod. Phys. A* **9**, 2411 (1994);
 [14] J. Alexandre and J. Polonyi, *Ann. Phys. (N.Y.)* **288**, 37 (2001); J. Alexandre, J. Polonyi, and K. Sailer, *Phys. Lett. B* **531**, 316 (2002).
 [15] D. F. Litim, *Phys. Lett. B* **486**, 92 (2000); *Phys. Rev. D* **64**, 105007 (2001); *J. High Energy Phys.* **11** (2001) 059.
 [16] D. F. Litim, *Phys. Rev. Lett.* **92**, 201301 (2004); D. F. Litim and T. Plehn, *Phys. Rev. Lett.* **100**, 131301 (2008).
 [17] J. M. Pawłowski, D. F. Litim, S. Nedelko, and L. von Smekal, *Phys. Rev. Lett.* **93**, 152002 (2004).
 [18] T. R. Morris, *J. High Energy Phys.* **07** (2005) 027.
 [19] O. J. Rosten, arXiv:1003.1366.
 [20] J. M. Pawłowski, *Ann. Phys. (N.Y.)* **322**, 2831 (2007); C. S. Fischer, A. Maas, and J. M. Pawłowski, *Ann. Phys. (N.Y.)* **324**, 2408 (2009).
 [21] D. F. Litim, J. M. Pawłowski, and L. Vergara, arXiv:hep-th/0602140.
 [22] J. Zinn-Justin, *Quantum Field Theory and Critical Phenomena* (Clarendon, Oxford, 1989).
 [23] I. Ichinose and H. Mukaida, *Int. J. Mod. Phys. A* **9**, 1043 (1994).
 [24] S. W. Pierson and O. T. Valls, *Phys. Rev. B* **61**, 663 (2000).
 [25] V. L. Berezinskii, *Zh. Eksp. Teor. Fiz.* **61**, 1144 (1971) [*Sov. Phys. JETP* **34**, 610 (1972)]; J. M. Kosterlitz and D. J. Thouless, *J. Phys. C* **6**, 1181 (1973).
 [26] Daniel F. Litim, *Nucl. Phys. B* **631**, 128 (2002).
 [27] R. D. Ball, P. E. Haagensen, J. I. Latorre, and E. Moreno, *Phys. Lett. B* **347**, 80 (1995); D. F. Litim, *Phys. Lett. B* **393**, 103 (1997); K. Aoki, K. Morikawa, W. Souma, J. Sumi, and H. Terao, *Prog. Theor. Phys.* **99**, 451 (1998); S. B. Liao, J. Polonyi, and M. Strickland, *Nucl. Phys. B* **567**, 493 (2000); J. I. Latorre and T. R. Morris, *J. High Energy Phys.* **11**

- (2000) 004; F. Freire and D.F. Litim, *Phys. Rev. D* **64**, 045014 (2001); L. Canet, B. Delamotte, D. Mouhanna, and J. Vidal, *Phys. Rev. D* **67**, 065004 (2003); *Phys. Rev. B* **68**, 064421 (2003); D.F. Litim, *J. High Energy Phys.* **07** (2005) 005; C. Bervillier, B. Boisseau, and H. Giacomini, *Nucl. Phys.* **B789**, 525 (2008); **801**, 296 (2008); S. Nagy and K. Sailer, *Ann. Phys. (N.Y.)* **326**, 1839 (2011).
- [28] J. Polchinski, *Nucl. Phys.* **B231**, 269 (1984).
- [29] J. Alexandre, V. Branchina, and J. Polonyi, *Phys. Lett. B* **445**, 351 (1999); C. Wetterich, *Nucl. Phys.* **B352**, 529 (1991).
- [30] I. Nándori, S. Nagy, K. Sailer, and A. Trombettoni, *J. High Energy Phys.* **09** (2010) 069; V. Pangon, S. Nagy, J. Polonyi, and K. Sailer, *Phys. Lett. B* **694**, 89 (2010); V. Pangon, [arXiv:1008.0281](https://arxiv.org/abs/1008.0281).
- [31] A.O. Gogolin, A.A. Nersisyan, and A.M. Tsvelik, *Bosonization and Strongly Correlated Systems* (Cambridge University Press, Cambridge, England, 1998); K.B. Efetov, C. Pépin, and H. Meier, *Phys. Rev. Lett.* **103**, 186403 (2009).
- [32] H. Gies and L. Janssen, *Phys. Rev. D* **82**, 085018 (2010).